Optimal design of panel speaker array with omnidirectional characteristics

Mingsian R. Bai[a] and Kuochan Chung
Department of Mechanical Engineering, National Chiao-Tung University, 1001 Ta-Hsueh Road, Hsin-Chu 300, Taiwan, Republic of China

(Received 31 August 2001; accepted for publication 31 July 2002)

A panel speaker system intended for a projection screen is developed. Like other sound sources with large dimension, the panel speaker has a beaming problem in high frequencies. To alleviate the problem, panel speakers are integrated into an array, with optimal electronic compensation for omnidirectional response and array efficiency. The heart of the design procedure is a three-stage optimization scheme involving two nonlinear and nonconvex objectives. The process is interactive, allowing the array coefficients to be tailored so that the specifications of directional response can be met. The optimal design of panel speaker array is then implemented by using a multichannel digital signal processor. In addition, a Hilbert transformer is required to produce the quadrature components of the array coefficients. A small array and a large matrix were constructed to validate the implemented array signal processing system. The experimental results indicate that, without degradation of efficiency, the proposed optimization technique in conjunction with electronic compensation is effective in attaining omnidirectional radiation property. [DOI: 10.1121/1.1509435]

PACS numbers: 43.38.Ar [SLE]

I. INTRODUCTION

This work focuses on the development of a projection screen which is composed of panel speakers. This system is intended for applications such as oral presentation, public addressing, or home theater. The system integrates both the audio and video functions into one unit, which may provide certain advantages over conventional systems. The main reason for using panel speakers lies in the flatness and compactness, which makes them well suited for the application as a projection screen. In general, a large and properly designed panel speaker is less directional in high frequencies than conventional cone speakers. However, a detailed electroacoustic analysis[1] revealed that this desirable property of panel speaker comes at the expense of efficiency. Furthermore, like other sound sources with large dimension, the panel speaker will still suffer from a peculiar beaming problem at coincidence angles in high frequencies if the radiating area is large.[2] As a solution to the above problem, this paper presents a speaker array approach, using an idea that contradicts the original distributed mode concept of panel speakers. We use small panels which are as light and stiff as possible to produce coherent but directional sound beams. Then, using electronic compensation and digital signal processing, we seek to achieve simultaneously omnidirectional response and array efficiency. If individual elements are identical, then the proposed beamforming technique also is applicable to arrays of conventional loudspeakers. The analysis and design of conventional loudspeaker arrays can be found in the literature.[3–6] It is also pointed out by the reviewer that a sound and light spectacle in Mexico used an array of panel speakers as the projection screen. This technology, invented by Sound Advance, is similar to a conventional cone speaker in as much as it uses a voice coil assembly.[7] However, it uses a flat diaphragm molded from expanded polystyrene, which allows the user to flush mount it inside a wall or ceiling in ''invisible'' fashion.

The design of an omnidirectional array boils down to finding a set of array coefficients that gives rise to a ''flat spectrum'' in the wave number space. For a linear array with real coefficients, direct inversion of an all-pass flat spectrum will apparently lead to the trivial solution: only one single element is active at the origin. This case corresponds to an array with very poor efficiency. Hence, two approaches have been proposed to avoid running into the dilemma between flat spectrum and array efficiency. One approach is to introduce a phase function into the directional response. The Bessel array and the quadratic phase array (QPA) are based on this idea.[6] The array gains in the QPA are purely phase compensation in quadratic forms. Another approach[8] is to choose a white-noise-like sequence with low correlation property, e.g., the Barker code, the Huffman code, and the maximum flatness sequence to produce a flat spectrum of array radiation pattern.

Different from the earlier approaches, an optimization technique is proposed in this paper to find array coefficients that maximize two cost functions: flatness and efficiency. This problem turns out to be a nonlinear and nonconvex problem for which it is generally very difficult to locate the global optimum. Hence, instead of finding the global optimum, we are content with the solution of a three-stage suboptimal problem. The design process is interactive, allowing us to tailor the array coefficients so that the specifications of directional response can be met. The array coefficients thus found are generally complex numbers, which entail the implementation of a Hilbert transformer.[9–11] The Hilbert

[a]Electronic mail: msbai@cc.nctu.edu.tw

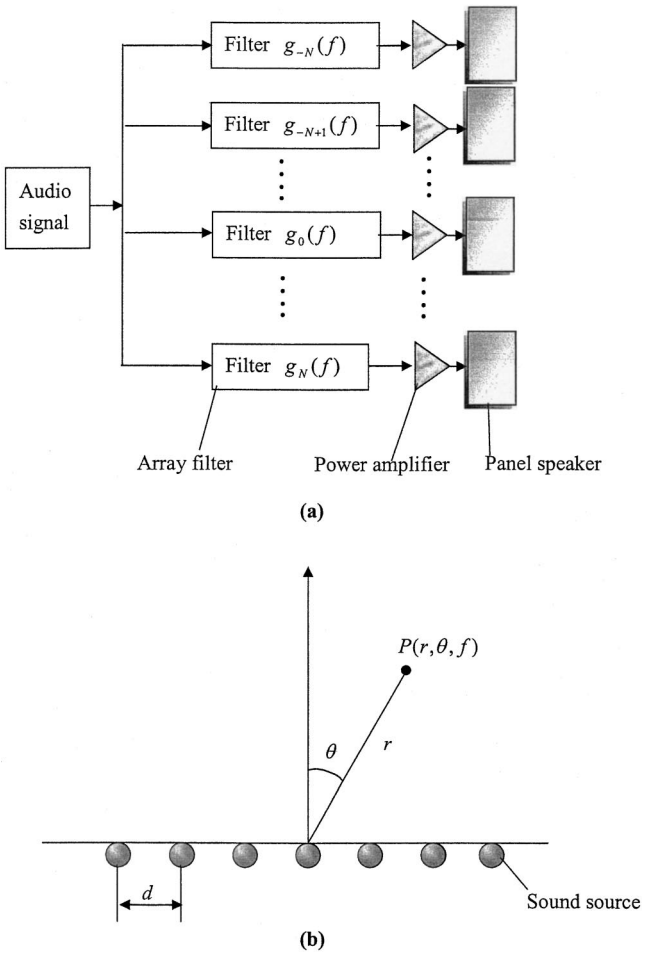

FIG. 1. A uniform linear array. (a) The schematic of a panel speaker array; (b) the array geometry.

transformer can be implemented in either IIR or FIR filter;[9] we will only discuss the latter approach.

A 5×1 panel speaker array and a 3×3 panel speaker array were constructed for experimental verification. Signal processing and electronic compensation are carried out by using a multichannel digital signal processor (DSP). Results will be compared and discussed with regard to an uncompensated array and the array obtained using the proposed optimization technique.

II. FAR-FIELD MODEL FOR UNIFORM LINEAR ARRAYS

A panel speaker array is schematically shown in Fig. 1(a). Audio signals are processed, often digitally, by a bank of filters before feeding to the power amplifiers and panel speakers. With reference to the geometry of Fig. 1(b), the far-field pressure radiated by a source array with $2N+1$ equally spaced elements can be expressed as[6,12]

$$P(r,\theta,f)=A(f,\theta)R(f,r)B(f,\theta), \tag{1}$$

where d is the spacing between two adjacent speakers, $r \gg d$ is the distance between the array center and a far-field observation point, θ is the angle measured from the normal to the array, f is the frequency, c is the sound speed, $A(f,\theta)$ is the radiation pattern of each source, $R(f,r)=r^{-1}\exp(j2\pi fr/c)$ represents the spherical spreading, $B(f,\theta)$ is the *array pattern*, defined as

$$B(f,\theta)=\sum_{n=-N}^{N} g_n(f)e^{j(2\pi nfd\sin\theta/c)}, \tag{2}$$

with $g_n(f)$ being the array coefficient of the nth element. Using the array filters, one is able to manipulate the array pattern to obtain the desired directional response.

Hereafter, we further restrict the array coefficients $g_n(f)$ to be frequency-independent, complex constants, g_n. The array pattern can then be written as

$$B(u)=\sum_{n=-N}^{N} g_n e^{jnu}, \tag{3}$$

where $u=2\pi fd\sin\theta/c$ is a dimensionless angle. Inspection of Eq. (3) reveals that the array pattern is essentially the frequency response of an FIR filter with coefficients g_n. That is, the design problem of an omnidirectional array can be regarded as the design of an FIR all-pass filter. For latter use, define the angular spectrum

$$S(u)=\|B(u)\|_2^2, \tag{4}$$

where $\|\ \|_2$ denotes the 2-norm, and the autocorrelation

$$R(k)=\sum_{n=-\infty}^{\infty} g_n g_{k-n}^{*}, \tag{5}$$

where k is the array index, g_n has a compact support within $[-N,N]$, "*" denotes complex conjugate. It can be shown that the angular spectrum is the Fourier transform of the autocorrelation, i.e.,

$$S(u)=\sum_{k=-N}^{N} R(k)e^{-jku}. \tag{6}$$

III. OBJECTIVES AND CONSTRAINTS

As mentioned earlier, the design goal of our problem is to find an array with omnidirectional characteristics and good efficiency. In this section, these design objectives will be formulated as two performance indices: *spectral flatness* and *array efficiency*.

A. Array efficiency

The array efficiency of a $(2N+1)\times 1$ array is defined as

$$\eta=\frac{R(0)}{(2N+1)|\mathbf{g}|_\infty}, \tag{7}$$

where $\mathbf{g}=\{g_n|-N\leqslant n\leqslant N, n\in N\}$, $|\mathbf{g}|_\infty=\max\{g_n|-N\leqslant n\leqslant N\}$ is the infinity norm of $\mathbf{g}$, and

$$R(0)=\sum_{n=-N}^{N}|g_n|^2=\frac{1}{2\pi}\int_{-\pi}^{\pi}S(u)du, \tag{8}$$

where the Parseval theorem has been invoked. Array efficiency is thus the mean-squared array gains normalized by $|\mathbf{g}|_\infty$. The physical meaning of the array efficiency can be interpreted as the degree of participation of active array elements. The efficiency will be close to unity if most array elements are active with full power (large gain values g_n).

B. Spectral flatness

For the same array, the merit factor, or the spectral flatness, is defined as[12,13]

$$F=\frac{R^2(0)}{\Sigma_{k\neq 0}|R(k)|^2}. \tag{9}$$

Using Eq. (6), we have

$$\frac{1}{2\pi}\int_{-\pi}^{\pi}S(u)du=\int_{-\pi}^{\pi}\sum_{k=-N}^{N}R(k)e^{jku}\,du=R(0). \tag{10}$$

According to the Parseval's relation, we have

$$\sum_{k=-N}^{N}|R(k)|^2=\frac{1}{2\pi}\int_{-\pi}^{\pi}S^2(u)du. \tag{11}$$

Substituting Eqs. (10) and (11) into Eq. (9) gives

$$F=\frac{(\int_{-\pi}^{\pi}S(u)du)^2}{2\pi\int_{-\pi}^{\pi}[S^2(u)-R^2(0)]du}. \tag{12}$$

The denominator of F can also be written as

$$\int\ [S^2(u)-R^2(0)]du=\int_{-\pi}^{\pi}[S(u)-R(0)]^2du. \tag{13}$$

From Eqs. (12) and (13), the spectral flatness F is the ratio of the mean-square spectrum over the spectral variance. An array with omnidirectional response tends to have large spectral flatness.

C. Constraints

Unfortunately, the aforementioned objective functions are not sufficient to reach a unique solution because any array coefficients differing within a scaling and/or a rotation will lead to identical F and η. This fact will be detailed in the following analysis.

Let $\mathbf{C}$ and $\mathbf{R}$ be the sets of real numbers and imaginary numbers, respectively. Suppose an array coefficient set $\mathbf{g}_1$ can be obtained from another set $\mathbf{g}=\{g_n|-N\leqslant n\leqslant N\}$ by a magnitude scaling r and a finite rotation u_0, i.e.,

$$\mathbf{g}_1=T(r,u_0,\mathbf{g})=\{rg_ne^{-jn\delta}|-N\leqslant n\leqslant N,r\in\mathbf{C},u_0\in\mathbf{R}\}. \tag{14}$$

Then, it is not difficult to verify the spectrum of the new coefficients

$$S_1(u)=|r|^2S(u+u_0). \tag{15}$$

The spectrum is scaled by a factor $|r|^2$ and shifted in u axis by u_0. Furthermore, the spectral flatness and array efficiency remain invariant under the transformation $T(r,u_0,g)$, i.e.,

$$F_1=F,\quad \eta_1=\eta, \tag{16}$$

and both coefficient sets are considered "equivalent." Consequently, additional constraints are needed to resolve this nonuniqueness problem. These constraints are derived from the following theorem. *Theorem*: For a $(2N+1)\times 1$ array, consider an array coefficient set $\mathbf{g}=\{g_n|-N\leqslant n\leqslant N\}$, with

$$|\mathbf{g}|_\infty=|g_0|. \tag{17}$$

Using the equivalent transformation of Eq. (14), the array coefficient set $\mathbf{g}$ can always be transformed into a "reduced" array coefficient set $\mathbf{J}$ given by

$$\mathbf{J}=\{J_n|J_n\in\mathbf{C},\ |J_n|\leqslant 1,\ -N\leqslant n\leqslant N,\ J_0=1\ \text{ and }\ \angle J_0=\angle J_1=0\} \tag{18}$$

Proof:

Let $r_0=e^{-j\angle g_0}/|\mathbf{g}|_\infty$, $\delta_0=\angle g_0-\angle g_1$, and

$$\mathbf{J}=T(r_0,\delta_0,g)=\left\{J_n=\frac{1}{|g|_\infty}g_ne^{j(\angle g_n-\angle g_0+n(\angle g_0-\angle g_1))}|J_n\in\mathbf{C},\ -N\leqslant n\leqslant N\right\}. \tag{19}$$

Substituting Eq. (17) into (19) leads to: $J_0=1$, $J_1=|g_1/g_0|$, and $|J|=|g_n/g_0|\leqslant 1$. Hence,

$$\mathbf{J}=\{J_n|J_n\in\mathbf{C},\ |J_n|\leqslant 1,\ -N\leqslant n\leqslant N,\ J_0=1\ \text{ and }\ \angle J_0=\angle J_1=0\},$$

which is Eq. (18). Q.E.D.

Thus, on the basis of the theorem, the feasible solution set of the array design problem can be dramatically reduced by imposing the following "fundamental constraints" in optimization:

$$g_0=1,\ \angle g_0=\angle g_1=0\ \text{ and }\ |g_n|\leqslant 1,\ -N\leqslant n\leqslant N. \tag{20}$$

Under this constraint, the maximum magnitude of array gain never exceeds unity.

IV. THE THREE-STAGE OPTIMIZATION PROCEDURE

In this section, an optimization technique is proposed to find array coefficients that maximize the aforementioned two cost functions: flatness and efficiency. Unfortunately, this problem turns out to be a nonlinear, nonconvex, and multiobjective problem for which it is generally very difficult and time-consuming to locate the global optimum. Hence, instead of finding the global optimum, we seek to find a suboptimal solution by using a three-stage optimization scheme—two stages for single-objective optimization and one stage for weighting two objectives.

A. The first stage: Phase optimization

To reiterate, the goal for the array design is to find array coefficients with high array efficiency and flat spectrum. For high efficiency, the magnitude of each array coefficient should be close to unity. For flat spectrum, the array coefficient set should be a random sequence with low correlation property. Putting these two statements together, one may conclude that the desired array coefficient set should be a random sequence satisfying two conditions: $|g_n|\approx 1$ and $\angle g_n$ is a random number over $[0,2\pi]$. Thus, in the first stage of optimization, we restrict the magnitude of each array coefficient at a "full efficiency" state, i.e., $|g_n|=1$, and adapt the phases as randomly as possible. The optimization problem in this stage can be stated as

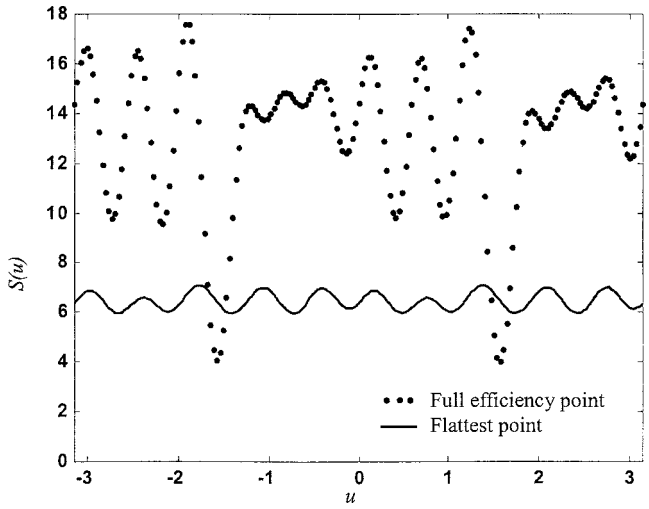

FIG. 2. The angular spectra at the full efficiency point and the flattest point for the 13×1 optimal array.

$$\underset{\theta_k \in R, -N \leqslant k \leqslant N}{\text{Max}} \quad F = \frac{R^2(0)}{\Sigma_{k \neq 0} R^2(k)}, \tag{21}$$

subject to the aforementioned fundamental constraints, and the ''full efficiency constraint,'' defined as

$$|g_k| = 1, \quad -N \leqslant k \leqslant N. \tag{22}$$

In this setting, the optimization in the first stage has only a single objective, spectral flatness. The *constrained steepest descent* (CSD)[14] method is employed to find the local maximum, or the ''full efficiency point.''

However, the result of the search is quite sensitive to initial conditions because the problem is nonlinear and nonconvex. As motivated by the characteristics of the optimal array, we thus adopted a heuristic but efficient approach and assigned random numbers to the phases as the initial guess. A simulation result obtained using the first-stage optimization for a 13×1 array is shown in Fig. 2. This simulation took approximately 1 min on a personal computer. The result was found by performing the first-stage optimization 20 times and selecting the flattest pattern as the full efficiency point. The step size of optimal search starts at 0.3 and decreases for convergence. Each optimization converged within 100 iterations. The calculated array coefficients are listed in Table I. It can be seen from the result that the angular spectrum fluctuates randomly since spectral flatness is not optimized in this stage.

B. The second stage: Magnitude and phase optimization

In this stage, both magnitude and phase of array coefficients are adjusted to further improve spectral flatness. After phase adapting, the only way to obtain more flatness is to adjust the magnitude of array coefficients. In effect, such optimization procedure is a ''tapering'' process of magnitude to get a broader and flatter spectrum, at the cost of array efficiency. The optimal problem in this stage is formulated as follows:

TABLE I. The array coefficients for the 13×1 optimal array at (a) the full efficiency point and (b) the flattest point.

Array index	(a)	(b)
−6	$\exp(j0.06)$	$0.21\exp(-j1.27)$
−5	$\exp(-j1.05)$	$0.51\exp(-j2.10)$
−4	$\exp(-j1.81)$	$0.58\exp(-j2.10)$
−3	$\exp(-j0.63)$	$0.72\exp(-j1.67)$
−2	$\exp(-j1.41)$	$1.00\exp(-j2.40)$
−1	$\exp(j3.07)$	$0.76\exp(j3.13)$
0	1	1
1	1	0.76
2	$\exp(j1.43)$	$1.00\exp(j2.40)$
3	$\exp(-j2.55)$	$0.73\exp(-j1.48)$
4	$\exp(j1.78)$	$0.58\exp(j2.08)$
5	$\exp(-j2.05)$	$0.50\exp(-j1.05)$
6	$\exp(-j0.10)$	$0.21\exp(j1.25)$
Flatness	18.74	360
Efficiency	1	0.50

$$\underset{\theta_k \in R, -N \leqslant k \leqslant N}{\text{Max}} \quad F = \frac{R^2(0)}{\Sigma_{k \neq 0} R^2(k)}, \tag{23}$$

subject to the fundamental constraints. The initial guess is the full efficiency point found in the last stage. The optimization in this stage is a nonlinear and nonconvex problem with one objective, flatness. CSD is used to find the suboptimal solution that is called the ''flattest point.''

The example of the 13×1 array is used again for the second-stage optimization. The result corresponding to the flattest point is also shown in Fig. 2. The array coefficients are listed in Table I. If the status of each iteration in this optimization stage is recorded, a trade-off can be observed between the flatness and efficiency. The search path for the 13×1 array is shown in Fig. 3. It can be seen in the plot that flatness is a monotonically increasing function of efficiency. The curve is terminated at both ends by the flattest point and the full efficiency point, respectively. The search path is

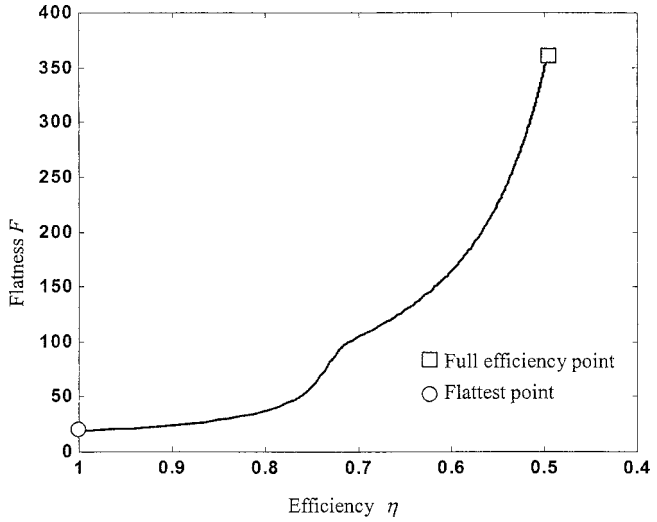

FIG. 3. The search path of efficiency and flatness for the 13×1 optimal array.

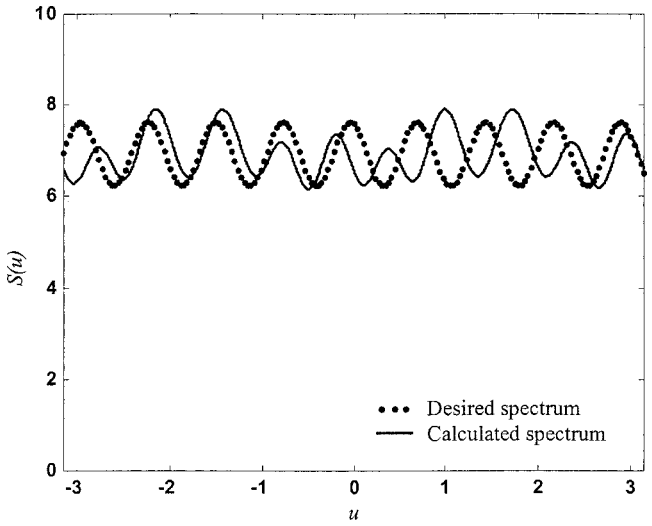

FIG. 4. The desired spectrum vs calculated spectrum for the 13×1 optimal array ($F=200$) found in the third stage.

stored in the computer for final tuning of the efficiency and flatness.

C. The third stage: Tuning of efficiency and flatness

As shown in Fig. 3, the search path for the array lies within the window

$$0.50 \leqslant \eta \leqslant 1, \tag{24}$$

and

$$19.68 \leqslant F \leqslant 360, \tag{25}$$

which renders the reachable performance limit in the design. In the third stage, the following template is employed as the desired spectrum:

$$S_d(u) = R_d(0) + A_{\text{ripple}} \sin u/T, \tag{26}$$

where $R_d(0)$ and A_{ripple} represent, respectively, the mean and the ripple size of the desired spectrum. For example, let $R_d(0)/A_{\text{ripple}}=10$. Substituting Eq. (26) into Eq. (12), the corresponding flatness should be

$$F_d = 2(R_d/A_{\text{ripple}})^2 = 200. \tag{27}$$

Using the search path in Fig. 3, one can find the corresponding efficiency to be 0.56. Recall the definition of array efficiency

$$\eta = R_d^2(0)/2N+1 = 0.56, \tag{28}$$

where $N=6$ for a 13×1 array. Solving Eqs. (27) and (28) yields $R_d(0)=7.30$ and $A_{\text{ripple}}=0.73$, based on which the desired spectrum is given by

$$S_d(u) = 7.28 + 0.728 \sin \frac{u}{T}. \tag{29}$$

If the result is acceptable, the corresponding array coefficients will be retrieved from the computer and the actual spectrum will be calculated. Otherwise, one should select another $R_d(0)/A_{\text{ripple}}$ and repeat this optimization stage. The desired spectrum and the actual spectrum for the example are compared in Fig. 4. Two spectra have similar ripple size and spectrum mean. The flow chart of the optimization with three stages is shown in Fig. 5.

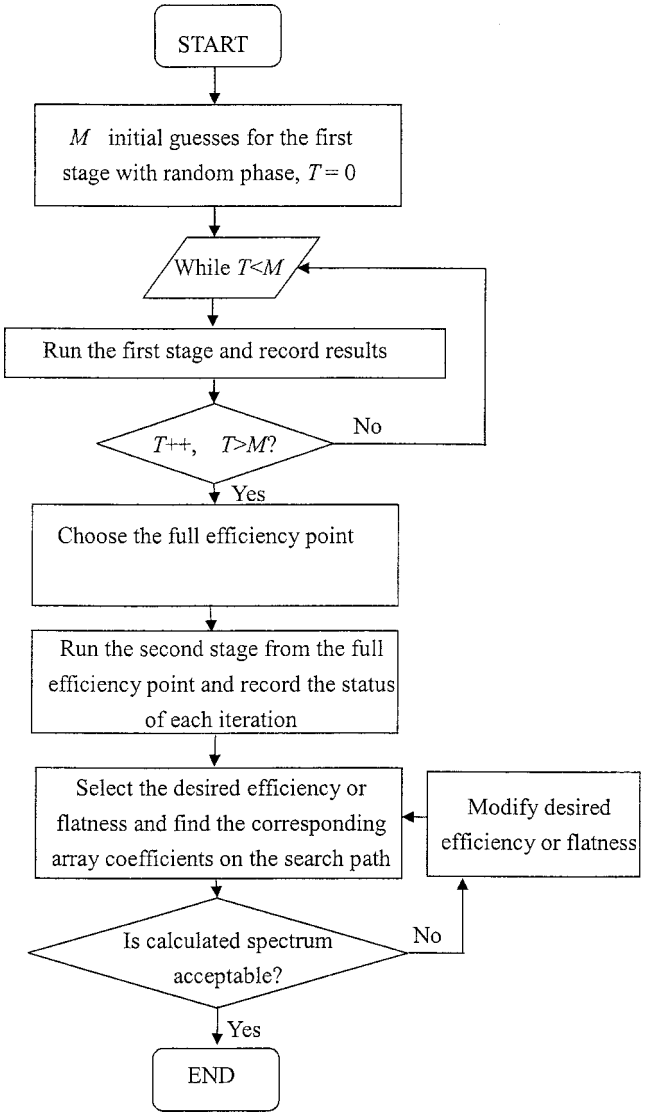

FIG. 5. The flow chart of the optimization procedure.

D. QPA array versus the optimal array

To justify the proposed technique, the 13×1 array designed using our optimization method is compared to the QPA array ($z=18$) where z is the shape factor. The array gains in the QPA are purely phase compensation in quadratic forms, $z(1-|\theta|/\pi)\theta/\pi$. The details of the QPA array can be found in Ref. 6. The array coefficients used in this simulation are listed in Table II. The angular spectra in Fig. 6 show that the spectrum of our array appears flatter than that of the QPA array. This is also reflected in Table II, where the calculated flatness is 11.5 vs 114.9 for the QPA array and our array, respectively, with identical efficiency.

V. EXPERIMENTAL INVESTIGATIONS

Two panel speaker arrays are constructed for experimental verification of the proposed array signal-processing techniques. In this section, a technical, but critical, issue in

TABLE II. The comparison of 13×1 QPA ($z=18$) and the 13×1 optimal array when the optimal array and QPA has the same efficiency.

Array index	QPA ($z=18$)	Optimal array
−6	0.74	0.35 exp(−j0.78)
−5	−0.78	0.61 exp(−j1.78)
−4	0.96	0.66 exp(−j1.92)
−3	−1.00	0.90 exp(−j1.22)
−2	0.45	1.00 exp(−j2.09)
−1	0.67	0.90 exp(j3.09)
0	−0.86	1
1	−0.67	0.94
2	0.45	1.00 exp(j2.03)
3	1.00	0.88 exp(−j2.02)
4	0.96	0.62 exp(j1.79)
5	0.78	0.59 exp(−j1.52)
6	0.74	0.37 exp(j0.57)
Flatness	11.53	114.9
Efficiency	0.63	0.63

implementing complex array coefficients shall be addressed, followed by hardware implementation of a 5×1 small array and 3×3 large array.

A. The implementation of complex array coefficients

As noted earlier, the resulting array coefficients g_n obtained using the proposed optimization techniques are generally complex. Although they are constants in nature, the approximation of which calls for the use of frequency-dependent filters

$$g_n(\omega)\approx \mathrm{Re}\{g_n\}+j\ \mathrm{Im}\{g_n\}, \tag{30}$$

where ω is the digital frequency, n is the array index, and $j=\sqrt{-1}$. The implementation of the filters is schematically shown in Fig. 7(a). The relationship between the input a_n and output b_n is given as

$$A(e^{j\omega})=[\mathrm{Re}\{g_n\}+H(e^{j\omega})\mathrm{Im}\{g_n\}]B(e^{j\omega}), \tag{31}$$

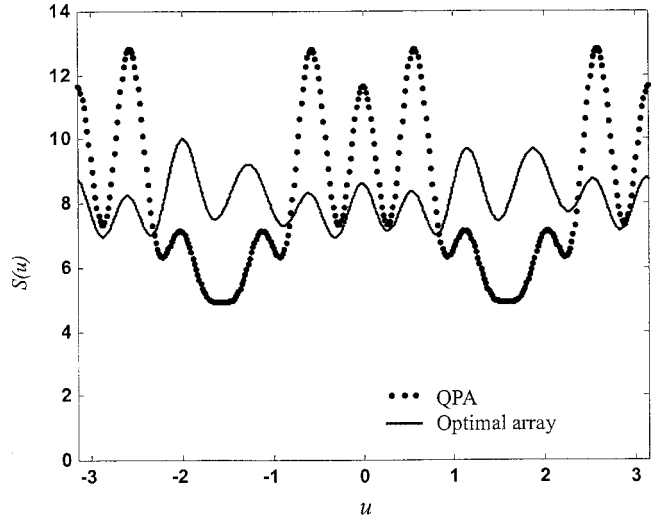

FIG. 6. The spectra of the QPA ($z=18$) and the optimal array (13×1), where both arrays have equal efficiency.

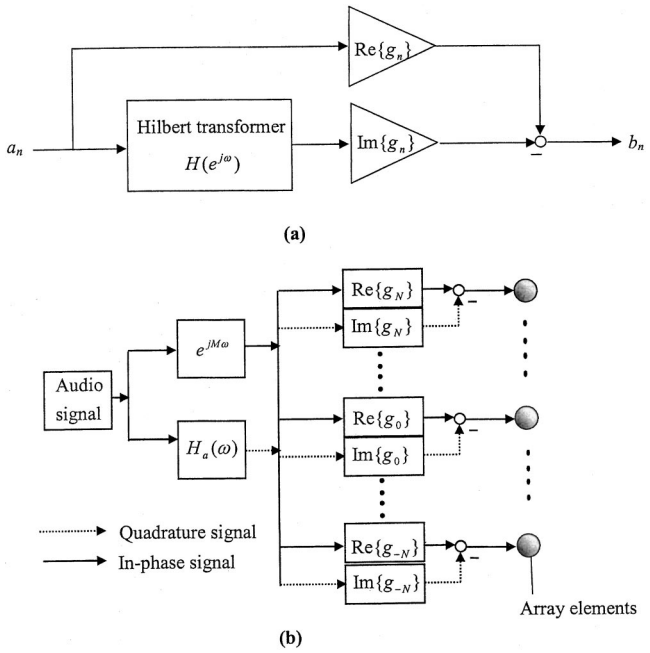

FIG. 7. The implementation diagram of complex array coefficients. (a) Single-channel array filter and the Hilbert transformer; (b) multichannel implementation.

where $A(e^{j\omega})$ and $B(e^{j\omega})$ are discrete Fourier transforms of a_n and b_n, respectively. The *Hilbert transformer*[9] $H(e^{j\omega})$ serves to generate a quadrature component. The frequency response of an ideal Hilbert transformer is

$$H(e^{j\omega})=\begin{cases} -j, & 0\leqslant\omega\leqslant\pi \\ j, & -\pi\leqslant\omega<0, \end{cases} \tag{32}$$

and the associated impulse response $h[n]$ is

$$h[n]=\begin{cases} \dfrac{2}{\pi}\dfrac{\sin^2(\pi n/2)}{n}, & n\neq 0 \\ 0, & n=0, \end{cases} \tag{33}$$

which is apparently noncausal. Hence, a delay of M samples with truncation should be introduced to approximate the ideal Hilbert transformer

$$H_a(e^{j\omega})=\begin{cases} e^{-j(M\omega+\pi/2)}, & 0\leqslant\omega\leqslant\pi \\ e^{-j(M\omega-\pi/2)}, & -\pi\leqslant\omega<0. \end{cases} \tag{34}$$

The frequency response of the modified array filter then becomes

$$g_n(\omega)\approx e^{-jM\omega}\{\mathrm{Re}\{g_n\}+j\ \mathrm{Im}\{g_n\}\}=e^{-jM\omega}g_n. \tag{35}$$

Note that no waveform distortion will arise due to the pure delay. Figure 7(b) shows the implementation in more detail. Using the implementation shown in Fig. 7(b) and substituting Eq. (35) into (2), we have

$$B(\theta,\omega)=e^{-jM\omega}\sum g_n e^{j2\pi fd\sin\theta/c}, \tag{36}$$

where $f=f_s\omega/2\pi$, f_s is the sampling frequency, f is analog frequency, and ω is digital frequency. Hence, the system in Fig. 7(b) yields an array pattern with the same magnitude response as the desired pattern. The Hilbert transformer

can be implemented by either an FIR[9] filter or an IIR[10,11] filter. In this work, we chose to use the FIR implementation. The Kaiser window approximation for a Hilbert transformer of order M takes the form[9]

$$h[n]=\begin{cases}\dfrac{I_o\{\beta(1-[(n-n_d)/n_d]^2)^{1/2}\}}{I_o(\beta)} \\ \quad\times\left\{\dfrac{2}{\pi}\dfrac{\sin^2[\pi(n-n_d)/2]}{n-n_d}\right\}, & 0\leqslant n\leqslant M \\ 0, \quad \text{otherwise.}\end{cases} \tag{37}$$

In the equation, $n_d=M/2$. It is noted that Hilbert transform will introduce frequency-dependent delay and result in some waveform distortion.

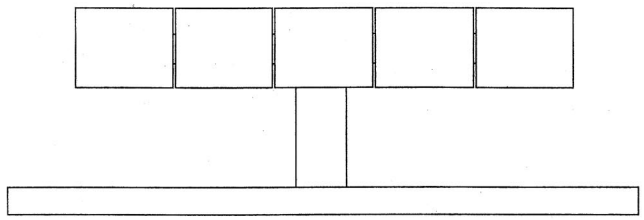

(a)

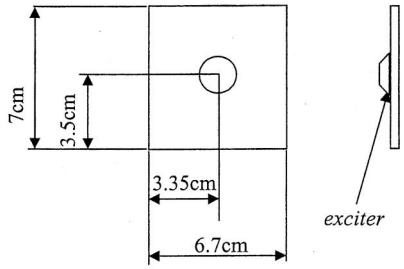

(b)

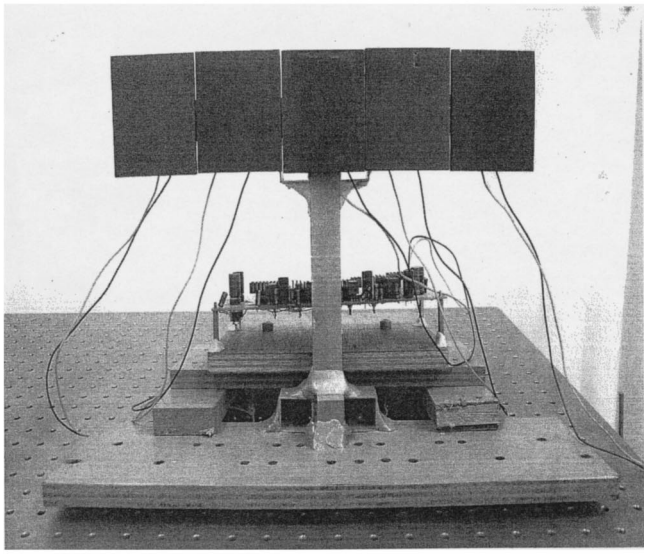

(c)

FIG. 8. The small panel speaker array. (a) Configuration of the 5×1 panel speaker array; (b) dimensions of panel speakers and the location of exciter; (c) the photo of the 5×1 panel speaker array.

B. The experimental result of a 5×1 linear panel speaker array

Although the ultimate goal of this work was to develop the large panel speaker array, we use a small array to verify the far-field behavior because of the limitation of current measuring environment. A 5×1 panel speaker array is constructed for experimental verification. The system consists of using PU-foam panel speakers, array signal-processing unit, a monitoring microphone, data acquisition unit, and a stepping motor unit. The dimensions and structure of the 5×1 panel speakers are shown in Figs. 8(a) and (b). The size of each rectangular panel is $7\times6.7\ \text{cm}^2$ and the spacing between adjacent speakers, $d=6.7$ cm. Each panel is driven by an electromagnetic exciter mounted on an aluminum frame. The photo of the array hardware is shown in Fig. 8(c).

The array signal processing is carried out by a floating-point DSP, TSM320C32 in conjunction with a multiple-channel IO module. Audio signals are fed to the array signal-processing unit, through AD conversion and power amplifi-

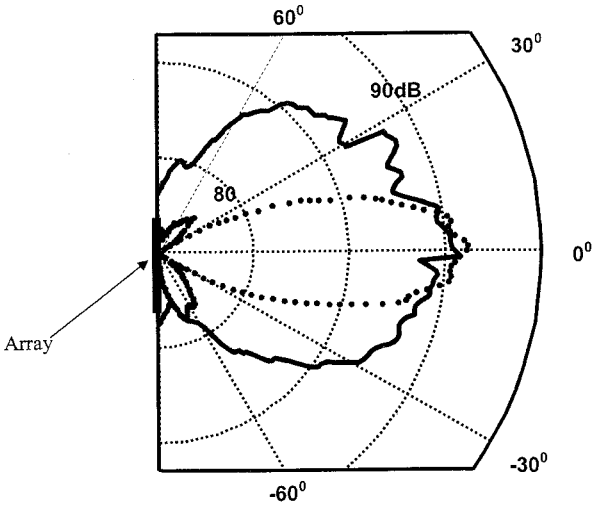

(a)

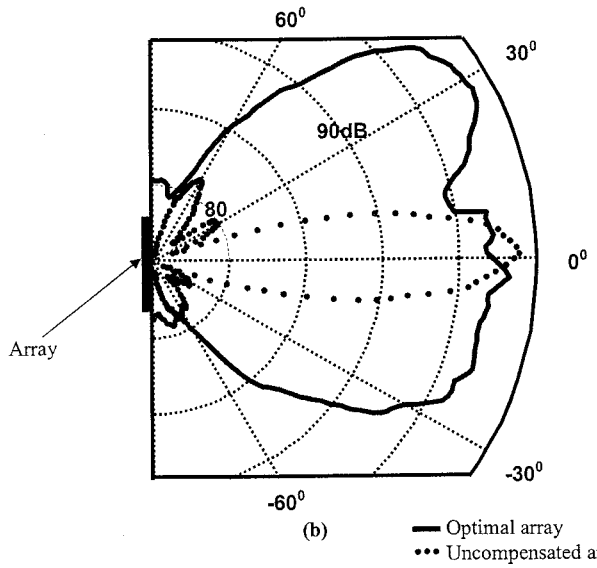

(b)

FIG. 9. The experimental results of directional response for the 5×1 panel speaker array at (a) 2 kHz and (b) 3 kHz.

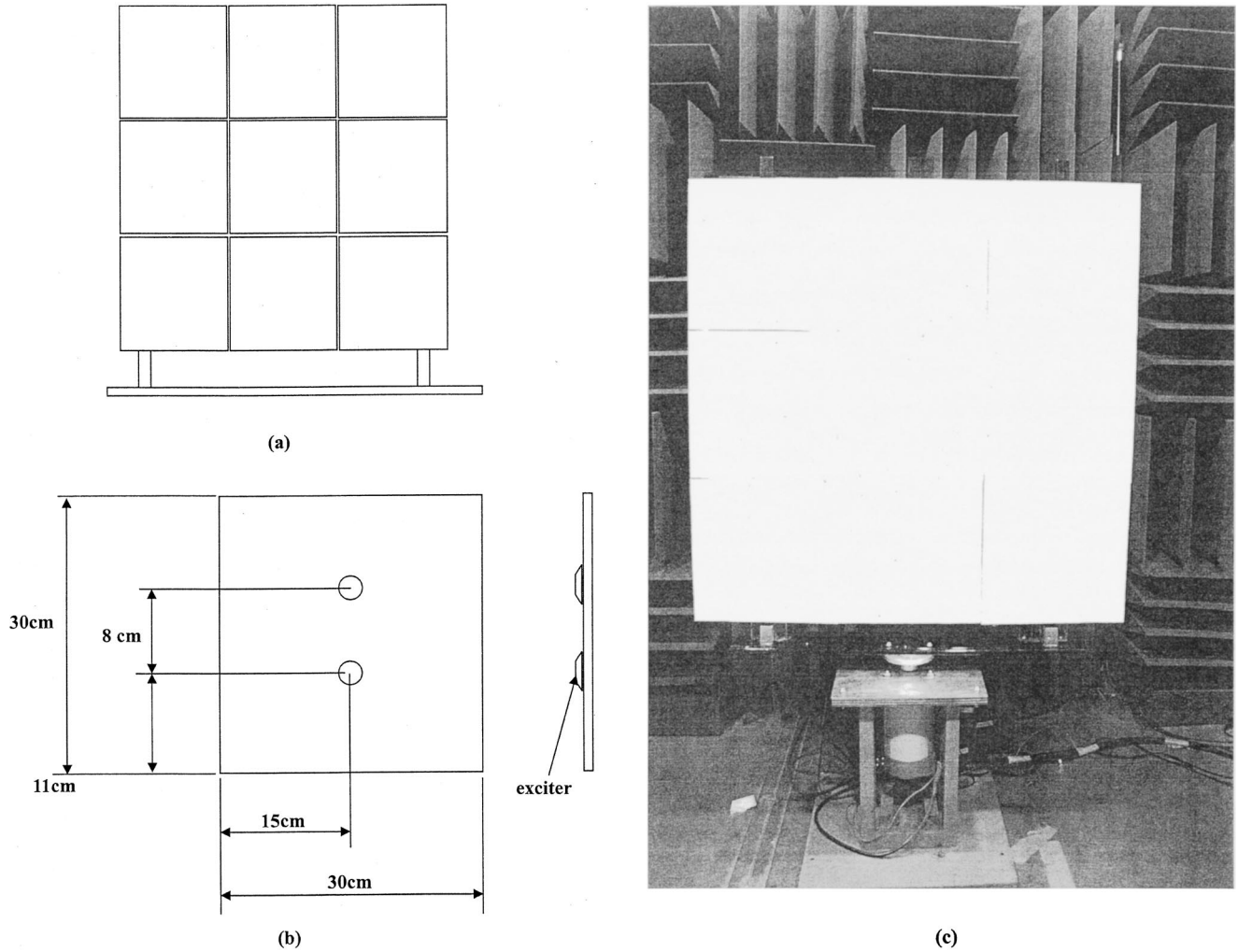

FIG. 10. The large panel speaker array of a projection screen. (a) Configuration of the 3×3 panel speaker array; (b) dimensions of panel speaker and the location of the exciter; (c) The photo of the 3×3 panel speaker array of a projection screen.

cation, and generate compensated signals for each channel of speaker. The monitoring microphone is situated 2 m from the center line of the array. The array is mounted on a turntable driven by the stepping motor so that directional responses of the array within $[-90°, 90°]$ can be recorded automatically, with every 1° increment. Necessary data acquisition/processing and motor control are all handled by the DSP as well. The experiments are conducted inside an anechoic chamber.

An experiment was conducted to compare the optimal panel speaker array to an uncompensated array ($g_n = 1, \forall n$). The optimal set of coefficients of the 5×1 array was found using the proposed optimization technique

$$\mathbf{g}_{\text{opt}} = \{-0.45, j, 1, j, -0.45\}. \tag{38}$$

The Hilbert transformer was implemented by a 100-tap FIR filter with a 50-sample delay, and sampling rate is 20 kHz. The directional response of the panel speaker array is measured at 2 and 3 kHz, respectively, on the horizontal plane of the array. Drastic differences can be observed in the experimental results of Fig. 9. The array is indicated in the figure. The uncompensated array indeed radiates a rather directional pattern, whereas the optimal array exhibits a relatively omnidirectional behavior.

C. The experimental result of a 3×3 panel speaker matrix

To further justify the panel speaker array, a large 3×3 matrix of the size of a projection screen is constructed using PU-foam panels, covered with glassy face skins. The dimensions and structure of the 3×3 panel speakers are shown in Fig. 10(a). The size of each panel is $30\times30\ \text{cm}^2$ and the spacing between adjacent speakers, $d = 30$ cm. The photo of the array hardware is shown in Fig. 10(b). Despite the matrix configuration, the array is based on one-dimensional compensation in the horizontal direction, which in our application is considered more important than the vertical direction. Each panel is driven by two electromagnetic exciters mounted on an aluminum frame. The three panels at each column are wired together to the same DSP output and six exciters are all in parallel connection. The rest of the details of experimental arrangement are identical to those of the 5×1 array.

An experiment was conducted to compare the optimal panel speaker array to an uncompensated array. The optimal

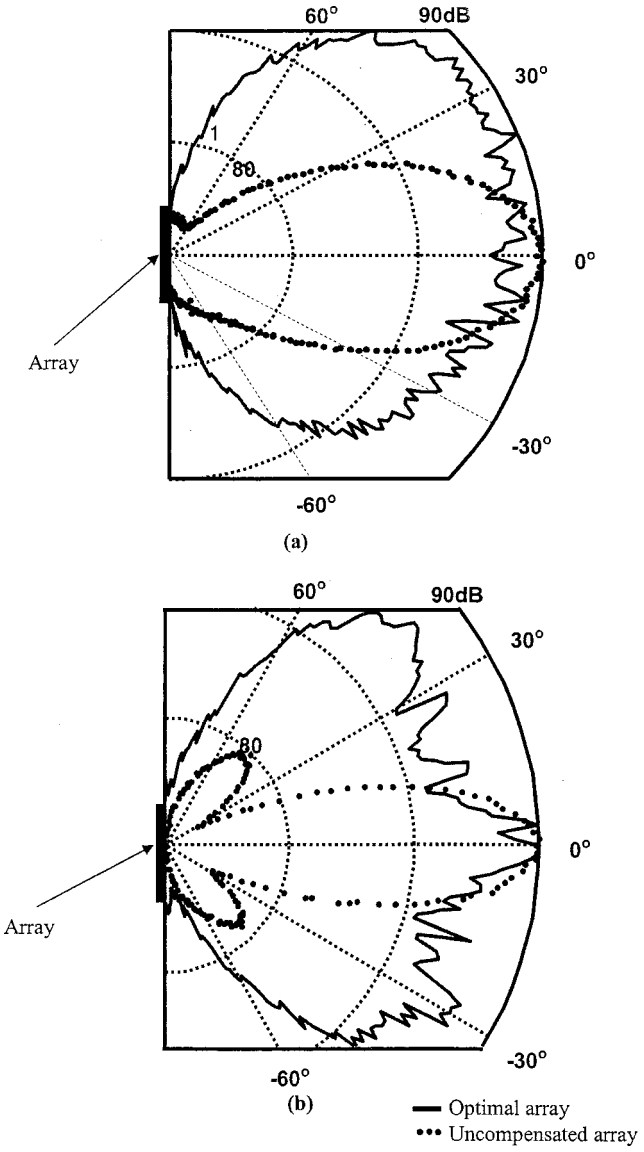

FIG. 11. The experimental results of directional response for the 3×3 panel speaker array at (a) 488 Hz and (b) 780 Hz.

set of coefficients of the 3×3 array was found using the proposed optimization technique

$$\mathbf{g}_{\text{opt}}=\{-0.45j,1,-045j\}. \tag{39}$$

The Hilbert transformer was implemented by a 150-tap FIR filter with a 75-sample delay, and sampling rate is 10 kHz. The directional responses of the panel speaker array is measured at 488 and 780 Hz, respectively, on the horizontal plane of the array. It is noted that in this large array experiment, we were able to investigate only near-field radiation pattern in our anechoic room. Similar to the case of small array, drastic difference can be observed in the experimental results of Fig. 11. The uncompensated array radiates a quite directive pattern, whereas the optimal array exhibits a relatively omnidirectional behavior.

VI. CONCLUSIONS

An important feature of this paper is the array optimization method, and the projection screen is a practical example of its use. Electronic compensation is employed to achieve omnidirectional response and array efficiency. Optimal design of array coefficients is computed by a three-stage optimization procedure that effectively solves the nonlinear and nonconvex problem. The process is interactive, allowing us to tailor the array coefficients to meet the design specifications. The array design obtained using the optimization technique has been implemented by using a multichannel DSP, where a Hilbert transformer is required to produce the quadrature components of the array coefficients. A small array and a large matrix were constructed to validate the implemented array signal-processing system. The experimental results obtained from the DSP-based system indicate that the optimally compensated panel speaker array exhibits omnidirectional radiation pattern without degradation of efficiency.

With regard to the use of panel speakers as projection screens, there are a few technical points to consider. These include the added brightness that can be achieved with a nonperforated screen, as well as the degree to which the response of large speaker arrays suffers from time smearing and poor stereo imaging.

Although the ultimate goal of this work was to develop the large array, we were unable to verify its far-field behavior due to the limitation of current measuring environment. Much work is continuing in improving the implementation as well as measurement of the large array for future research.

ACKNOWLEDGMENTS

Special thanks are due to the illuminating discussions with *NXT, New Transducers Limited*, UK. The work was supported by the National Science Council in Taiwan, Republic of China, under the project number NSC 89AFA06000714.

[1] M. R. Bai and T. Huang, "Development of Panel Loudspeaker System: Design, Evaluation and Enhancement," J. Acoust. Soc. Am. **109**, 2751–2761 (2001).
[2] L. E. Kinsler, A. R. Ffrey, A. B. Coppens, and J. V. Sanders, *Fundamentals of Acoustics* (Wiley, New York, 1982).
[3] D. L. Smith, "Discrete-Element Line Arrays—Their Modeling and Optimization," J. Audio Eng. Soc. **45**, 949–964 (1997).
[4] G. L. Augspurger, "Near-Field and Far-Field Performance of Large Woofer Arrays," J. Audio Eng. Soc. **38**, 231–236 (1990).
[5] D. G. Meyer, "Digital Control of Loudspeaker Array Directivity," J. Audio Eng. Soc. **32**, 747–754 (1984).
[6] R. M. Aarts and A. J. E. M. Janssen, "On Analytic Design of Loudspeaker Arrays with Uniform Radiation Characteristics," J. Acoust. Soc. Am. **107**, 287–292 (2000).
[7] *Sound Advance*, http://soundadvance.com/.
[8] G. F. M. Beenker, T. A. C. M. Claasen, and P. W. C. Hermens, "Binary Sequences with a Maximally Flat Amplitude Spectrum," Philips J. Res. **40**, 289–304 (1985).
[9] A. V. Oppenheim and R. W. Schafer, *Discrete-Time Signal Processing* (Prentice-Hall, Englewood Cliffs, NJ, 1989).
[10] Z. G. Jing, "A New Method for Digital All-Pass Filter Design," IEEE Trans. Acoust., Speech, Signal Process. **35**, 1557–1564 (1987).
[11] B. Gold, A. V. Oppenheim, and C. M. Radar, "Theory and Implementation of the Discrete Hilbert Transformer," in *Proc. Symp. Computer Processing in Communications*, Vol. 19 (Polytechnic, New York, 1970).
[12] D. F. Johnson and D. F. Dudgeon, *Array Signal Processing Concepts and Techniques* (Prentice-Hall, Englewood Cliffs, NJ, 1993).
[13] M. J. E. Golay, "The Merit Factor of Long, Low Autocorrelation Binary Sequences," IEEE Trans. Inf. Theory **28**, 543 (1982).
[14] J. S. Arora, *Introduction to Optimum Design* (McGraw-Hill, Singapore, 1989).